



# Particulate and gaseous pollutants in a petrochemical industrialized valley city, Western China during 2013–2016

Xi Zhou<sup>1</sup> · Tingjun Zhang<sup>1</sup> · Zhongqin Li<sup>2,3</sup> · Yan Tao<sup>1</sup> · Feiteng Wang<sup>2</sup> · Xin Zhang<sup>3</sup> · Chunhai Xu<sup>2</sup> · Shan Ma<sup>1</sup> · Ju Huang<sup>1</sup>

Received: 28 November 2017 / Accepted: 1 March 2018 / Published online: 20 March 2018  
© Springer-Verlag GmbH Germany, part of Springer Nature 2018

## Abstract

Airborne pollutant characteristics, potential sources, and variation trends of cause are investigated based on the hourly air concentrations of gaseous pollutants and particulate matter from 2013 to 2016 in Lanzhou. The mean concentration of SO<sub>2</sub>, NO<sub>2</sub>, CO, 8-hO<sub>3</sub>, PM<sub>2.5</sub>, and PM<sub>10</sub> was  $25.2 \pm 16.0 \mu\text{g m}^{-3}$ ,  $46.5 \pm 21.1 \mu\text{g m}^{-3}$ ,  $1.3 \pm 0.7 \text{mg m}^{-3}$ ,  $77.8 \pm 45.5 \mu\text{g m}^{-3}$ ,  $58.7 \pm 32.9 \mu\text{g m}^{-3}$ , and  $131.1 \pm 86.2 \mu\text{g m}^{-3}$ , respectively. The concentrations of SO<sub>2</sub>, PM<sub>10</sub>, and PM<sub>2.5</sub> present decreasing trends while NO<sub>2</sub>, CO, and O<sub>3</sub> present increasing trends. PM is the most frequent major pollutants with much higher value than standard limit. However, NO<sub>2</sub> pollution had obvious trends to reach the limit and was more serious in Lanzhou compared with other Chinese cities. Relationship between air pollutants and meteorological parameters suggested that lower primary pollutants were associated with higher wind speed from north and west. Modeled back trajectory demonstrated that the transport of air masses from the Hexi Corridor and Inner Mongolia was responsible for the high concentrations of the air pollutants in wintertime, and high PM<sub>10</sub> level in springtime was related to long-range transport of dust from desert areas of the Sinkiang and the Central Asia. Effects of local pollutant emissions and meteorological condition were preliminary analyzed. Improvement of air quality might be related to the decreasing of pollutant emissions due to strict emissions controls, and the contribution of meteorological condition was not explicit and should be further investigated.

**Keywords** Lanzhou · Gaseous pollutants · Particulate matter · Meteorological condition · Potential source

Responsible editor: Gerhard Lammel

**Electronic supplementary material** The online version of this article (<https://doi.org/10.1007/s11356-018-1670-6>) contains supplementary material, which is available to authorized users.

✉ Zhongqin Li  
lizq@lzb.ac.cn

- <sup>1</sup> Key Laboratory of Western China's Environmental Systems (Ministry of Education), College of Earth and Environmental Sciences, Lanzhou University, Lanzhou 730000, China
- <sup>2</sup> State Key Laboratory of Cryospheric Science/Tien Shan Glaciological Station, Northwest Institute of Eco-Environment and Resources, Chinese Academy of Sciences, Lanzhou 730000, China
- <sup>3</sup> College of Geography and Environmental Science, Northwest Normal University, Lanzhou, China

## Introduction

Rapid urbanization and industrial development have caused severe deterioration of the urban air quality in China. The air pollutants including gaseous pollutants and particulate matter have significant influences on climate, atmospheric environment, and human health (Ostro 2004; Kan et al. 2007; Lim et al. 2013; IPCC 2007). Ambient pollution of cities and rural areas was estimated to cause 7 million premature deaths (one in eight of total global deaths) worldwide in 2012. In 2014, 92% of the world population was living in the places where the WHO air quality guidelines levels were not met (WHO 2016). Seven out of the top 10 most polluted cities in the world are Chinese cities, and only five cities in China reached WHO air quality guidelines (Zhang and Crooks 2012). With the low visibility days and the increases of air pollution events in recent years, The State Council passed the revised Chinese

Ambient Air Quality Standards (CAAQS, Table S1 in the supplement), in which the limited value of NO<sub>2</sub> was further restricted and O<sub>3</sub> and PM<sub>2.5</sub> were added to the standard system from January 2013 based on GB3095-2012 (<http://hbj.new.cqcs.gov.cn/upfiles/2013-3/2013327153015207.pdf>). Furthermore, the Ministry of Environmental Protection (MEP) of China started to release the hourly mean concentrations of six criteria pollutants online, including SO<sub>2</sub>, NO<sub>2</sub>, O<sub>3</sub>, CO, PM<sub>2.5</sub>, and PM<sub>10</sub> at several monitoring sites of the major cities. The air quality data are necessary to comprehend current air pollutant conditions in many Chinese areas and can provide some useful information and scientific measures for local governments to solve pollution issues (Hu et al. 2014).

Lanzhou (36.05° N, 103.88° E) is a narrow valley city located in downwind areas of Taklimakan Desert and Hexi Corridor regions in northwestern China, and it is influenced considerably by mineral dust. In addition, it is an important industrial city characterized by large-scale oil refinery and petrochemical industry. The first photochemical smog in China was reported in Lanzhou in the 1970s, which has been widely known as the milestone of the modern air pollution research in China (Tang et al. 1989). There are ever-increasing petrochemical industries in the west of the city and the number of vehicles has increased from 0.34 to 1.05 million between 2008 and 2015 (Gansu Yearbook 2016). The combination of dust and anthropogenic pollution together with the undiffused terrain has caused Lanzhou to become one of the most heavily polluted cities in China and even around the world.

Nevertheless, in recent years, significant mitigation strategies have been taken to reduce air pollution such as central heating, traffic restriction, and regular watering on the streets. The air quality is improving in Lanzhou and even “Lanzhou Blue” has appeared. Air pollution in Lanzhou has been studied during the last decades (Ta et al. 2004; Wang 2011; Chu et al. 2008a, b; Wang et al. 2016). However, most of the studies only focus on one single pollutant or were limited in few months. Systematic knowledge of pollution characteristic in Lanzhou is still lacking compared with other Chinese cities and many cities outside China. Few studies involving simultaneous hourly data in Lanzhou for such six pollutants have been published since the standard was revised. We aim to fill the knowledge gap by using a 4-year (2013–2016) air quality data released by MEP. This study takes Lanzhou as a unique example for revealing the process of atmospheric pollutant variation, parsing potential sources, and preliminarily analyzing the cause. The detailed findings include those on (1) overview of air pollution in Lanzhou in recent years, (2) temporal and spatial variation patterns of six criteria pollutants, (3) comparisons with other Chinese sites, (4) relationship between air

pollutants and meteorological parameters, (5) source analysis by principal component analysis and back trajectory clustering analysis, and (6) preliminary analysis of cause.

## Methods

### Studying area

Lanzhou is in the downstream areas and on the transport path of the dust storms from the two areas: (a1) Taklimakan basin and Gobi Desert region and (a2) the Badain Jaran Desert and Hexi Corridor region. Lanzhou is located at a narrow (2–9 km width), long (40 km), NW-SE oriented valley basin with the mean elevation about 1600 m above the sea level, and it has four districts: Chengguan, Anning, Qilihe, and Xigu. Chengguan District is in the eastern of Lanzhou city, which is the metropolitan area including government, residence, and commerce. Anning District is in the north middle of Lanzhou city and Qilihe District is in the south middle of Lanzhou city; both are the mixed residential, semiworks, and cultivation (vegetables) areas. Xigu District is in the western of Lanzhou city, which is the petrochemical industrial area. The five sites in different districts reflect difference of potential sources of air pollution (Fig. 1); Lanyuan Hotel (LYH) in the Xigu District reflected industry sources, Lanzhou Railway Bureau (LRB) in Chengguan District reflected traffic intensity sources, Lanzhou Institute of Biology Products (LIBP) in Chengguan District reflected population density sources, Shengjian Worker Hospital (SWH) in Qilihe District reflected the mixed sources, and Yuzhong campus of Lanzhou University (YZ) was a reference point and reflected the geographical and climatic conditions.

### Data collection

The hourly mean concentration of Air Quality Index (AQI) and criteria pollutants (SO<sub>2</sub>, NO<sub>2</sub>, CO, 1-hO<sub>3</sub>, 8-hO<sub>3</sub>, PM<sub>2.5</sub>, and PM<sub>10</sub>) from January 18, 2013, to December 31, 2016, in Lanzhou were from the China National Environmental Monitoring Center (<http://106.37.208.233:20035/>). The concentrations of air pollutants of 113 major cities in 2015 were from National Bureau of Statistics of China (<http://www.stats.gov.cn/tjsj/nds/2016/indexch.htm>). Meteorological data were collected from Lanzhou surface meteorological station, including atmospheric temperature, pressure, relative humidity, wind speed, and direction. All the consolidated data was presented in Table 1.

Concentrations of the gaseous pollutants (SO<sub>2</sub>, NO<sub>2</sub>, O<sub>3</sub>, and CO) and particulate matters (PM<sub>2.5</sub> and PM<sub>10</sub>) were measured by the automated monitoring stations at each city. SO<sub>2</sub>,

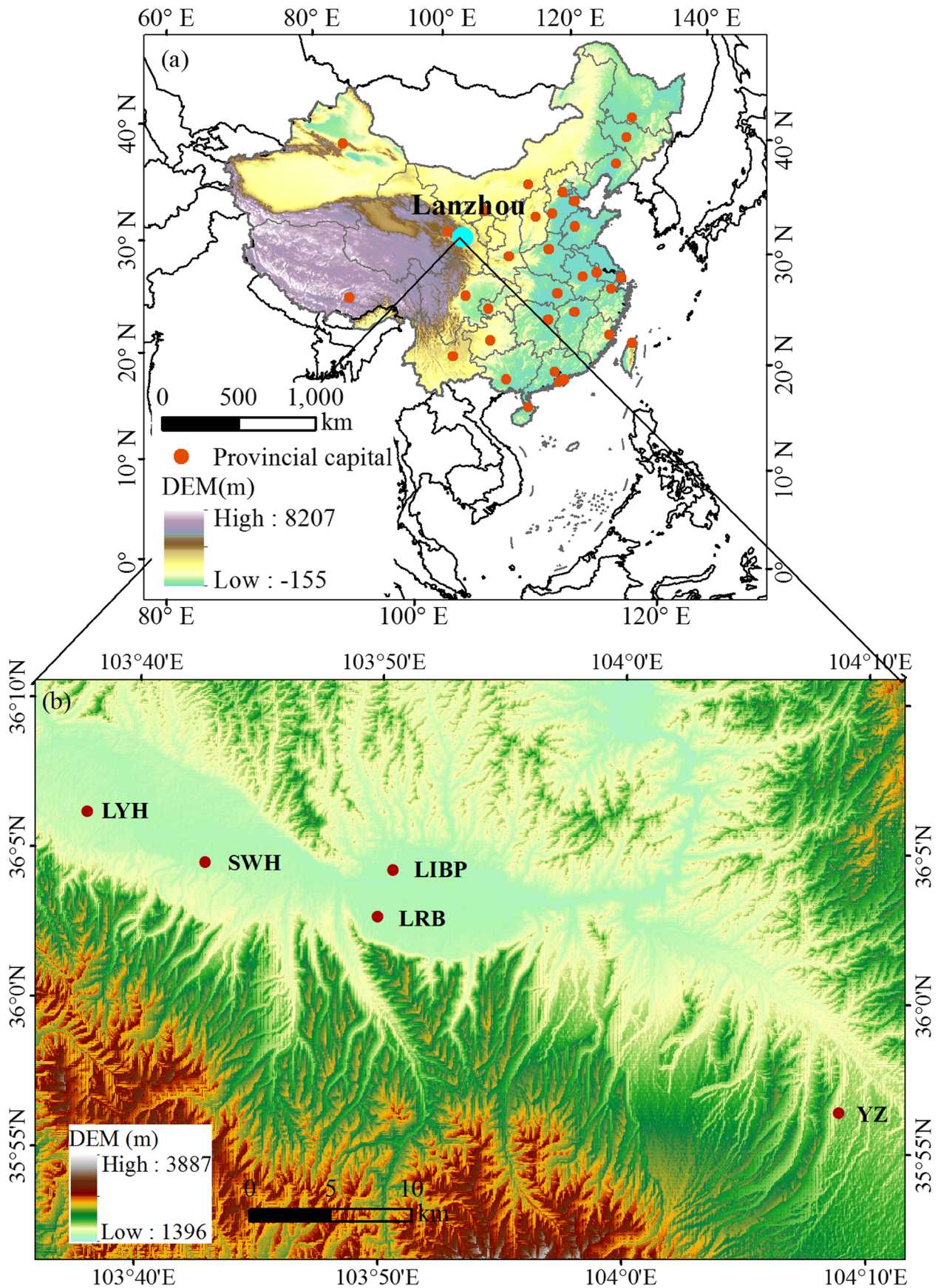


Fig. 1 Lanzhou. a Geography, a1 and a2 represent two high frequency areas of dust storms. b Topography

**Table 1** Statistical summary of six criteria pollutants and relevant meteorological parameters during 2013–2016

Year	Pollutant species (annually average ± SD (min-max))						Meteorological parameter					
	AQI	SO <sub>2</sub> (m/m <sup>3</sup> )	NO <sub>2</sub> (m/m <sup>3</sup> )	CO (m/m <sup>3</sup> )	8-hO <sub>3</sub> (µg/m <sup>3</sup> )	PM <sub>2.5</sub> (µg/m <sup>3</sup> )	PM <sub>10</sub> (µg/m <sup>3</sup> )	T (°C)	P (hPa)	WS (m/s)	RH (%)	
2013	117.0 ± 32.9 (41–500)	34.9 ± 17.9 (8–112)	35.9 ± 10.5 (7–101)	0.9 ± 0.5 (0.1–4.4)	77.4 ± 33.1 (14–462)	72.5 ± 20.3 (19–250)	154.3 ± 52.2 (37–882)	9.3 ± 10.2 (–12.3–25.4)	832.4 ± 5.0 (820–843)	1.7 ± 0.6 (0.5–4.8)	53.1 ± 19.7 (12–99)	
2014	95.1 ± 17.1 (38–358)	27.2 ± 10.5 (5–64)	46.3 ± 9.0 (9–136)	1.5 ± 0.4 (0.5–4.3)	63.1 ± 12.9 (8–221)	60.2 ± 13.6 (16–332)	124.8 ± 30.4 (36–1001)	7.8 ± 10.4 (–13.0–24.8)	831.8 ± 4.6 (822–847)	1.6 ± 0.6 (0.5–3.7)	58.2 ± 18.3 (17–96)	
2015	87.4 ± 12.7 (33–337)	20.2 ± 9.8 (4–75)	46.9 ± 8.2 (11–112)	1.4 ± 0.6 (0.5–4.2)	78.1 ± 21.2 (25–165)	48.8 ± 12.3 (17–143)	113.5 ± 21.3 (27–448)	8.4 ± 10.0 (–11.2–26.6)	833.0 ± 4.6 (818–846)	1.7 ± 0.5 (0.6–4.1)	56.6 ± 17.2 (18–97)	
2016	96.2 ± 29.9 (31–462)	18.7 ± 12.7 (4–62)	56.7 ± 18.2 (13–140)	1.3 ± 0.6 (0.5–4.2)	92.4 ± 27.3 (11–190)	53.6 ± 21.9 (13–223)	131.9 ± 54.6 (27–1199)	–	–	–	–	
Mean	98.9 ± 49.2 (31–500)	25.2 ± 16.0 (4–112)	46.5 ± 21.1 (7–141)	1.3 ± 0.7 (0.1–4.4)	77.8 ± 45.5 (8–462)	58.7 ± 32.9 (13–334)	131.1 ± 86.2 (27–1199)	7.84 ± 10.3 (–17.5–22.6)	832.8 ± 4.9 (819–849)	1.7 ± 0.59 (0.5–4.9)	55.1 ± 18.2 (12–99)	

NO<sub>2</sub>, and O<sub>3</sub> were measured by the ultraviolet fluorescence method (TEI, Model 43i from Thermo Fisher Scientific Inc., USA), chemiluminescence method (TEI Model 42i from Thermo Fisher Scientific Inc., USA), and the UV spectrophotometry method (TEI model 49i from Thermo Fisher Scientific Inc., USA), respectively. CO was measured using the nondispersive infrared absorption method and the gas filter correlation infrared absorption method (TEI, Model 48i from Thermo Fisher Scientific Inc., USA). PM<sub>2.5</sub> and PM<sub>10</sub> were measured by the micro oscillating balance method (TEOM from Rupprecht & Patashnick Co., Inc., USA) and the β-absorption method (BAM 1020 from Met One Instrument Inc., USA).

The data quality assurance was conducted based on HJ 630-2011 specifications (<http://kjs.mep.gov.cn/hjbhzbz/bzwb/other/qt/201109/W020120130585014685198.pdf>) before being released to the open website. The accuracy, consistency, and validity of the data have been checked based on some methods, as well as comparison with the previous data. In our study, the released data have been further processed to evaluate the pollution status in China. First, the data has no missing values, confirming the data completeness. Besides, the validity of the data has been demonstrated based on GB 3095-2012 specifications. Monthly averaged concentrations of six critical pollutants were calculated based on at least 25 daily average concentrations. The quality assurance and control procedure were also supplied in all cities and the gas analyzers were calibrated with standard gases once a week. To better confirm the quality of the data, reliability analysis was also performed. The results of reliability analysis indicated Cronbach’s alpha was 0.832 (> 0.6), suggesting the reliability of the data.

### Data analyses

#### AQI calculation

AQI was calculated by using pollutant concentration data (Table S2 in the supplement) and the following equation (linear interpolation):

$$IAQI_p = \frac{IAQI_H - IAQI_L}{BP_H - BP_L} (C_p - BP_L) + IAQI_L \tag{1}$$

$$AQI = \max\{IAQI_1, IAQI_2, IAQI_3, \dots, IAQI_n\} \tag{2}$$

where IAQI<sub>p</sub>—the index for pollutant *p*; C<sub>p</sub>—the rounded concentration of pollutant *p*; BP<sub>H</sub>—the breakpoint that is greater than or equal to C<sub>p</sub>; BP<sub>L</sub>—the breakpoint that is less than or equal to C<sub>p</sub>; IAQI<sub>H</sub>—the AQI value corresponding to BP<sub>H</sub>; IAQI<sub>L</sub>—the AQI value corresponding to BP<sub>L</sub>; and *n*—the pollutant item listed in Table S2 in the supplement.

### Trajectory cluster

Cluster analysis was used to categorize air backward trajectories into groups of similar history such as similar direction of advection and velocity of air movement. To gain the impact of transport on the air pollutants in Lanzhou, five-day backward air mass trajectories are conducted by using the NOAA HYSPLIT model and the NCEP/NCAR meteorological re-analysis dataset (Draxler and Rolph 2013). The model is run per day once for the sampling period at 500 m above ground level. The geographical coordinates were changed into *x*, *y* on a plane using the azimuthal equidistant projection with a central point with the geographical position of the Lanzhou station before the cluster analyses. The distortion associated with the projection had a secondary effect on the classification. The calculated Euclidean distances d<sub>ij</sub> between *i*-th trajectory and a mean *j*-th cluster trajectory are defined as follows:

$$d_{ij}^2 = \sum_{l=1}^{l=N\_level} \sum_{k=1}^{k=N\_hour} [(x_i - X_j)^2 + (y_i - Y_j)^2] \tag{3}$$

where *l*—number of trajectory level considered; *k*—index equal to air pass time from a given trajectory point to Lanzhou expressed in hours; *x<sub>i</sub>*, *y<sub>i</sub>*—coordinates on the plane of *k*-th point of the *i*-th trajectory reaching the *l*-th height above the station; and *X<sub>j</sub>*, *Y<sub>j</sub>*—coordinates on the plane of *k*-th point of an average trajectory of the *j*-th cluster reaching the *l*-th height above the station.

The algorithm minimized the following factor:

$$f = \sum_{j=1}^{j=N\_cl} \sum_{i=1}^{i=N\_j} d_{ij}^2 \tag{4}$$

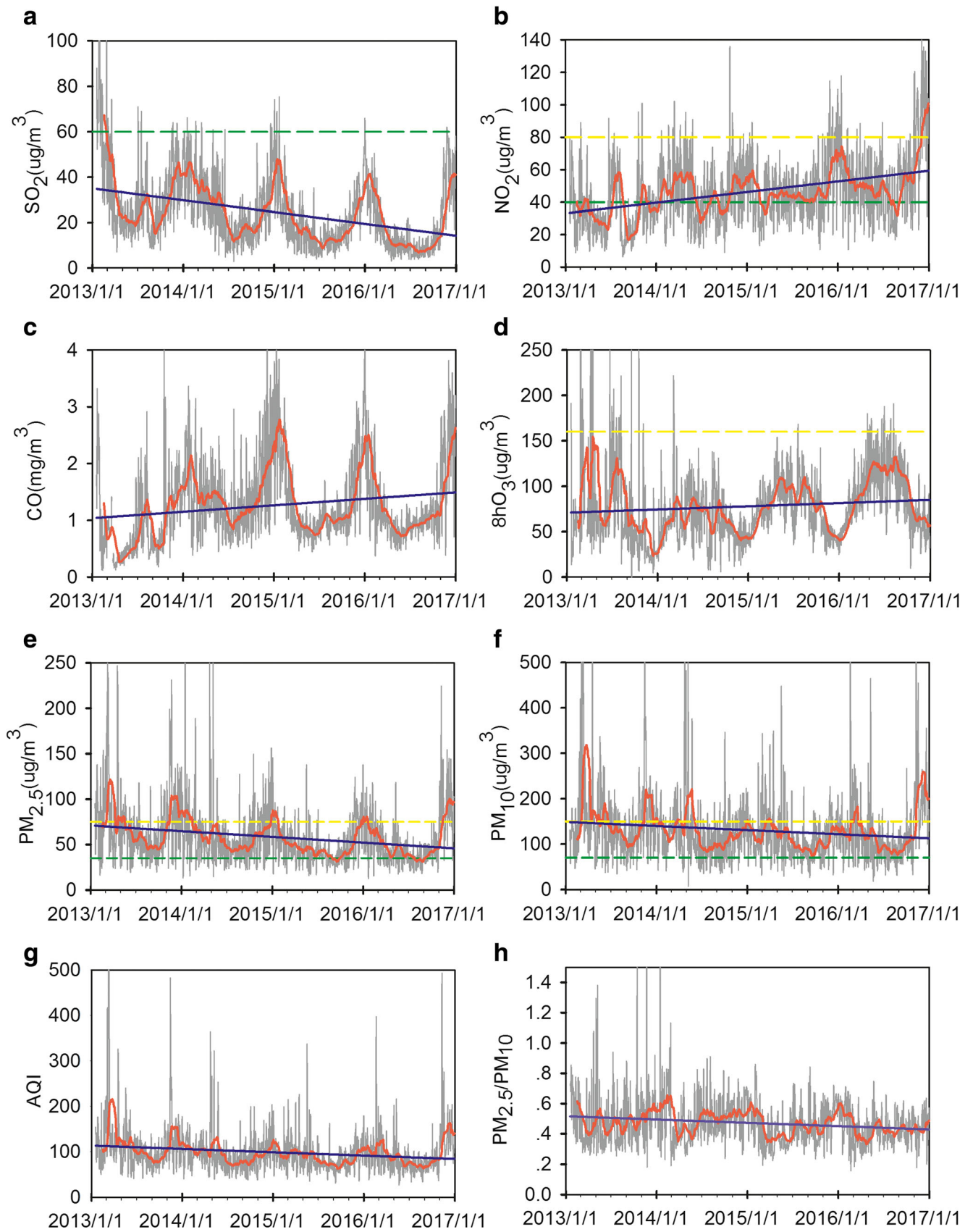
where *i* is a subsequent trajectory in *j*-th cluster, N<sub>cl</sub> is a number of clusters, and N<sub>j</sub> denotes a number of trajectories of the *j*-th cluster.

## Results and discussions

### Trend analysis of air pollutants

A statistical summary of the air quality and meteorological data during the entire study period (2013–2016) in Lanzhou is presented in Table 1. The average value of AQI, SO<sub>2</sub>, NO<sub>2</sub>, CO, 8-hO<sub>3</sub>, PM<sub>2.5</sub>, and PM<sub>10</sub> over the lasting 4 years was 98.9 ± 49.2, 25.2 ± 16.0 μg m<sup>-3</sup>, 46.5 ± 21.1 μg m<sup>-3</sup>, 1.3 ± 0.7 mg m<sup>-3</sup>, 77.8 ± 45.5 μg m<sup>-3</sup>, 58.7 ± 32.9 μg m<sup>-3</sup>, and 131.1 ± 86.2 μg m<sup>-3</sup>, respectively. PM was the most frequent

**Fig. 2** Plot of daily concentration of **a** SO<sub>2</sub>, **b** NO<sub>2</sub>, **c** CO, **d** 8-hO<sub>3</sub>, **e** PM<sub>10</sub>, **f** PM<sub>2.5</sub>, **g** AQI, and **h** PM<sub>2.5</sub>/PM<sub>10</sub> in Lanzhou between 2013 and 2016 (green dash lines represent annual mean concentration limit values; yellow represents daily)



major pollutants in Lanzhou, while CO and NO<sub>2</sub> were the second frequent major pollutants, which mainly are due to pollutant emission and the diffusion conditions in the atmospheric boundary layer, as well as the special events such as the sandstorm events (Liu et al. 2015).

To analyze the trends of pollutants, we computed the annual distribution using the 24-h moving average time series from 2013 to 2016 in Fig. 2. On average, decreasing trends of SO<sub>2</sub>, PM<sub>10</sub>, and PM<sub>2.5</sub> as well as increasing trends of NO<sub>2</sub>, CO, and O<sub>3</sub> demonstrated the air pollution pattern in Lanzhou. The horizontal dashed lines are referred as CAAQS Grade II standard, and yellow and green represented daily limit values and

annual limit values, respectively. AQI decreased by 1.45%. The level of SO<sub>2</sub> had a steadily decreasing trend by 5.12 μg m<sup>-3</sup> year<sup>-1</sup> and was lower than Grade II standard (150 μg m<sup>-3</sup>) all the years. The annual mean value of NO<sub>2</sub> increased from 35.9 ± 10.5 to 56.7 ± 18.2 μg m<sup>-3</sup> with a rate of 6.45 μg m<sup>-3</sup> year<sup>-1</sup>. The maximum daily value of NO<sub>2</sub> reached 140 μg m<sup>-3</sup>, which was 1.75 times the concentration of the Grade II standards. Most importantly, the NO<sub>2</sub>/SO<sub>2</sub> was 1.21 in 2013, which demonstrated the almost equal contribution of mobile and stationary sources, while the value increased to 4.08 in 2016, which suggested that the mobile origins became more influential. The increasing speed of CO

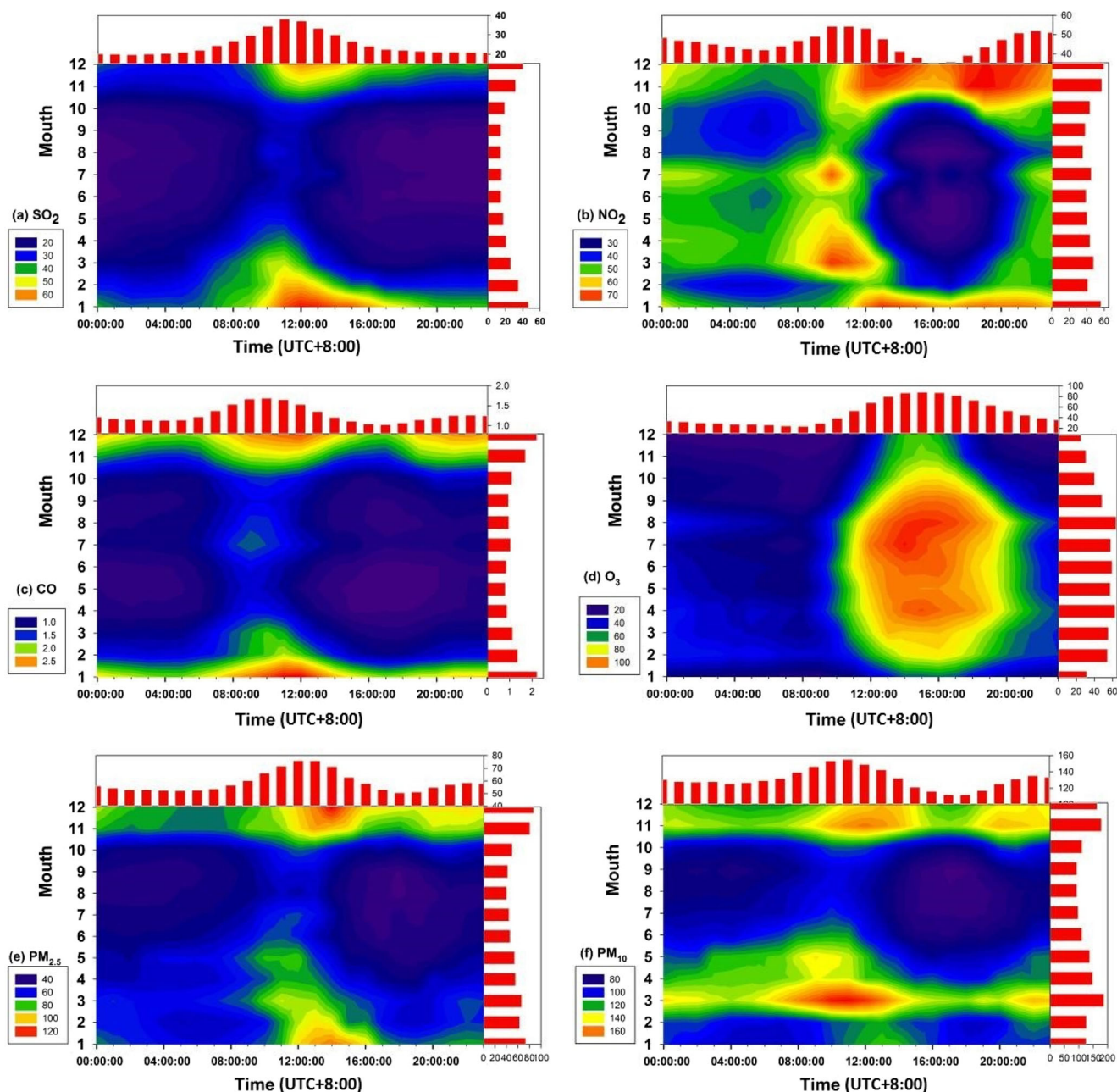


**Fig. 3** Gaseous concentration (a SO<sub>2</sub>, b NO<sub>2</sub>, c CO, and d O<sub>3</sub>) and particulate matter (e PM<sub>2.5</sub> and f PM<sub>10</sub>) distribution related to time (filled color)

concentration is  $0.11 \text{ mg m}^{-3} \text{ year}^{-1}$ . The CO concentration is clearly under the safe level except several days with poor meteorological condition in winter heating periods. O<sub>3</sub> was increased with a rate of  $3.48 \text{ } \mu\text{g m}^{-3} \text{ year}^{-1}$ , which pointed to worsening photochemical pollution.

The peak levels occurred in 2013 for PM<sub>2.5</sub> and PM<sub>10</sub>, but the enhanced trends were also recorded in 2016. PM<sub>2.5</sub> and PM<sub>10</sub> levels showed a decreasing trend with speed of 6.23 and  $8.95 \text{ } \mu\text{g m}^{-3} \text{ year}^{-1}$ , respectively. The PM<sub>2.5</sub>/PM<sub>10</sub> was used to identify sources since different sizes of airborne particles are probably from different sources. Low ratios (<0.6) are attributed to the preponderant contribution from dust storm from long-distance transport (Wang et al. 2014), while high ratios are attributed to secondary particulate formation of SO<sub>4</sub><sup>2-</sup>, NH<sub>4</sub><sup>+</sup>, NO<sub>3</sub><sup>-</sup>, and organics. The mean value of PM<sub>2.5</sub>/PM<sub>10</sub> in Lanzhou was lower than 0.47, which was lower than other Chinese regions. It suggests that Lanzhou in downstream regions of Taklimakan Desert and Hexi Corridor region was influenced by sand-dust storms easily (Chan and Yao 2008; Wang et al. 2009).

### Temporal variation of air pollutants

#### Seasonal variation

To establish the temporal variation of air pollution, the seasonal and diurnal variations during 2013–2016 were shown in Fig. 3. The concentrations of six air pollutants were separated to four seasons, spring (March–May), summer (June–August), fall (September–November), and winter (December–February).

High SO<sub>2</sub> concentration appeared in the winter with obvious periodical variation. The mean SO<sub>2</sub> in winter was greater than  $42 \text{ } \mu\text{g m}^{-3}$ . January was the peak month ( $51.1 \text{ } \mu\text{g m}^{-3}$ ). The greatest CO values were also observed during winter, and the peak month was December ( $2.2 \text{ mg m}^{-3}$ ). Summer is the season with the lowest SO<sub>2</sub> ( $< 15.2 \text{ } \mu\text{g m}^{-3}$ ) and CO ( $< 1.0 \text{ mg m}^{-3}$ ). NO<sub>2</sub> concentration exceeded Grade II ( $40 \text{ } \mu\text{g m}^{-3}$ ) in all seasons, but maximum NO<sub>2</sub> concentration was  $54.0 \text{ } \mu\text{g m}^{-3}$  in the winter and minimum NO<sub>2</sub> concentration was  $40.3 \text{ } \mu\text{g m}^{-3}$  in the summer. December was the peak month with a  $64.5 \text{ } \mu\text{g m}^{-3}$  mean NO<sub>2</sub>. Notably, SO<sub>2</sub>, CO, and NO<sub>2</sub> showed high value in winter largely due to household heating that usually starts in November and ends in the following March. But NO<sub>2</sub> and CO showed different pattern with SO<sub>2</sub> in diurnal variation, which suggested that NO<sub>2</sub> and CO are still effected by other anthropogenic activities, such as vehicle emission. Due to the photochemically active nature of NO<sub>2</sub>, which caused the chemical reaction cycle relating to ozone and other precursors, NO<sub>2</sub> values were lower in the summer. In opposite, the greatest O<sub>3</sub> occurs in the summer, and the mean O<sub>3</sub> was generally  $119.1 \text{ } \mu\text{g m}^{-3}$ . O<sub>3</sub> showed an opposite pattern probably due to high temperature and strong solar radiation intensity in summer, which is beneficial to the O<sub>3</sub> formation (Atkinson and Arey 2003).

The mean values of PM<sub>10</sub> and PM<sub>2.5</sub> were generally  $137.0$  and  $74.6 \text{ } \mu\text{g m}^{-3}$  in the winter, respectively. The peak month for PM<sub>10</sub>, however, was March ( $185.9 \text{ } \mu\text{g m}^{-3}$ ). The peak month for PM<sub>2.5</sub> concentrations was December ( $85.8 \text{ } \mu\text{g m}^{-3}$ ). The maximum wintertime PM concentrations were associated with the combustion for heating and with enhanced temperature inversion and more frequent

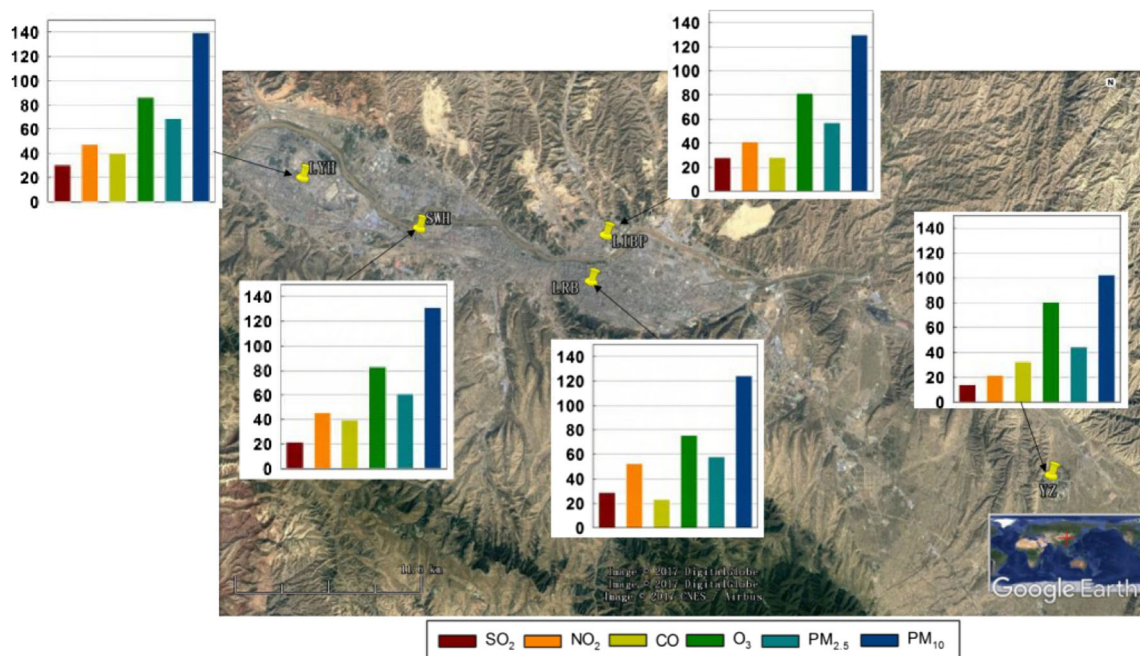


Fig. 4 Spatial concentration distribution of six pollutants in Lanzhou during 2013–2016 ( $\mu\text{g m}^{-3}$ , except CO  $0.1 \text{ mg m}^{-3}$ )

stagnant weather during the colder months, and these can lead to the accumulation of airborne particles and result in high particulate pollution episodes (He et al. 2001; Xia et al. 2006; Timonen et al. 2013). Meanwhile, high springtime  $PM_{10}$  concentrations always followed the maximum winter-time  $PM_{10}$  concentration, and this is probably due to special dust events (Wang et al. 2004). Certainly, the minimum  $PM$  concentrations in summer were related to the decrease of anthropogenic emissions for heating, more effective wet scavenging due to plentiful precipitation during summer monsoon, and the pollutant diffusion dilution on account of increased convection in a higher atmospheric mixing boundary layer (Choi et al. 2008; Titos et al. 2014).

### Diurnal variation

The  $SO_2$  concentrations increased from 6:00, followed by a peak value in 11:00 ( $38.1 \mu\text{g m}^{-3}$ ), then concentration decreased to low level at approximately 17:00. The lowest  $SO_2$

values ( $19.7 \mu\text{g m}^{-3}$ ) occurred at 3:00.  $NO_2$  daily cycles with a pattern were characterized by a rise at 7:00 and a morning maximum at 11:00, then concentrations decreased until 16:00, after which they rose until 22:00 (an evening peak).  $CO$  also displayed a pattern with a rise at 6:00 and a peak at 10:00 and a rise at 18:00 and a peak at 22:00. The morning peaks are caused by the increased anthropogenic activity during rush hour, and in the winter, domestic heating could result in high emission during nighttime.  $O_3$  concentration was greatest at the afternoon ( $\sim 16:00$ ) and lowest at the morning ( $\sim 8:00$ ). The lowest  $PM_{10}$  ( $111.8 \mu\text{g m}^{-3}$ ) and  $PM_{2.5}$  values ( $50.7 \mu\text{g m}^{-3}$ ) both occurred at 18:00, and the highest  $PM_{10}$  and  $PM_{2.5}$  levels were  $155.5 \mu\text{g m}^{-3}$  at 11:00 and  $76.1 \mu\text{g m}^{-3}$  at 12:00, respectively. Notably, the diurnal variation of  $PM_{10}$  and  $PM_{2.5}$  was similar to  $NO_2$  and  $CO$ , which indicated the important effect of traffic source on  $PM$  fractions.

Aside from emissions, this pattern probably caused by the variation of the atmospheric boundary layer height (ABLH) (Fig. S1 in the supplement), because the enhancement of

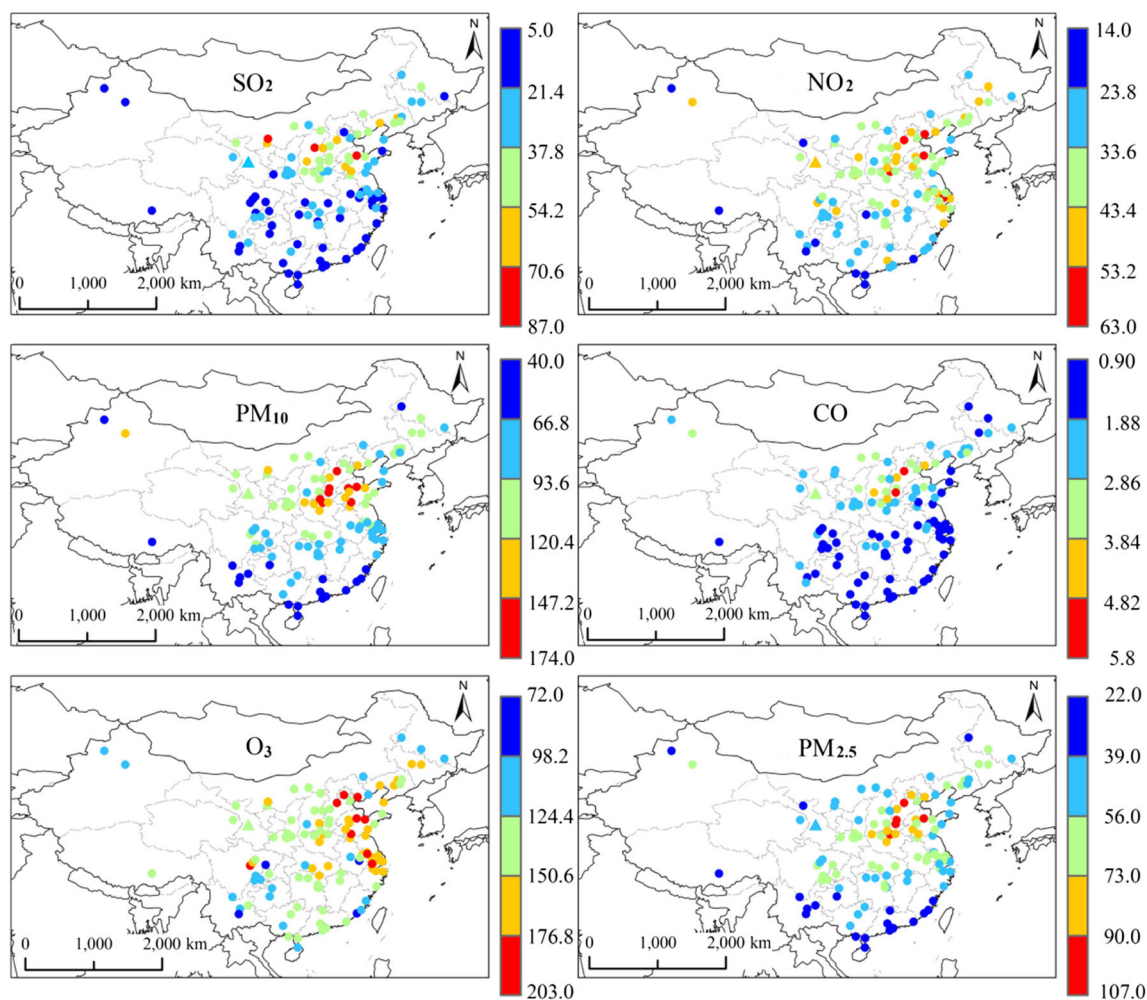


**Fig. 5** Average concentrations of six pollutants ( $\mu\text{g m}^{-3}$ , except  $CO \text{ mg m}^{-3}$ ) for 113 major cities in 2015 (the triangle represents Lanzhou, CO is the 95th percentile of daily mean concentration,  $O_3$  is the 90th percentile of daily maximum 8-h concentration)

ABLH supplies a larger volume and space for diluting pollutants and reducing its concentrations. The low pollutant concentrations in the afternoon were found due to the high ABLH and wind speed leading to better dispersion and dilution, which was consistent with studies of Guan et al. (2017) and Zhao et al. (2016). Other low value occurred at night, and reduced citizen travel and dry deposition to remove particle result in lower pollutant concentrations. In summer, dry deposition with higher humidity probably causes the minimum pollutant concentration overnight, but in winter, although dry deposition increased at night, the pollutant concentrations still show an increasing trend due to heating.

**Spatial variation of air pollutants**

The spatial variations during 2013–2016 in Lanzhou were shown in Fig. 4. The highest mean concentration was detected in Xigu District and the lowest concentration was observed in Yuzhong; the spatial variation stated that air pollution in sub-urb was low due to less human activities. For SO<sub>2</sub> concentrations, the industrial site LYH in Xigu District (year mean value 30.4 μg m<sup>-3</sup>) was higher than other sites. In the traffic site LRB in Chengguan District, levels of NO<sub>2</sub> were high with mean value 52.3 μg m<sup>-3</sup> exceeding the established annual limit value of 40 μg m<sup>-3</sup> (CAAQS), indicating the strong effect of traffic emissions on air quality. The lowest O<sub>3</sub> concentrations were measured in the traffic sites LRB (75.4 μg m<sup>-3</sup>) since in traffic and urban areas with elevated

fresh emissions of NO, some of the O<sub>3</sub> present is depleted while oxidizing NO to NO<sub>2</sub>. A clear intra-city trend was observed for CO with higher values in the industrial site LYH due to its direct association with the emissions from the incomplete combustion of fossil fuels and biofuels. PM<sub>2.5</sub> and PM<sub>10</sub> were high at the industrial site (PM<sub>2.5</sub> 68.9 μg m<sup>-3</sup>, PM<sub>10</sub> 139.4 μg m<sup>-3</sup>), exceeding the established annual limit values of 35 μg m<sup>-3</sup> for PM<sub>2.5</sub> and 75 μg m<sup>-3</sup> for PM<sub>10</sub> (CAAQS). However, the mixed site SWH in Qilihe District also has a high PM concentration, which might be because the site was influenced by atmospheric transport from Xigu District nearby. Therefore, spatial variation of air pollutants was not only influenced by local emission but also by meteorological condition; local emission can cause high primary pollutant concentration in emission areas such as SO<sub>2</sub> and NO<sub>x</sub> emission, while meteorological condition such as wind can cause relatively high secondary pollutant concentration in nearby emission sources areas.

**Comparisons with other Chinese sites**

Figure 5 provides a comparison of pollutant concentrations of the 113 major cities of China in 2015. Nationwide, the most polluted cities was principally concentrated in the North China Plain, while slightly polluted cities are mainly concentrated in southern China. PM<sub>2.5</sub> was the frequent major pollutants in China, followed by PM<sub>10</sub> and O<sub>3</sub>. In North and West regions,

**Table 2** Pearson correlation coefficients between six pollutants and meteorological parameters

	SO <sub>2</sub>	NO <sub>2</sub>	CO	PM <sub>2.5</sub>	PM <sub>10</sub>	8-hO <sub>3</sub>
<b>WS</b>						
Spring	-0.095	-0.265	-0.210	0.117	0.178	0.022
Summer	-0.060	-0.328	-0.258	-0.119	0.009	-0.011
Fall	0.049	-0.088	-0.115	-0.072	0.057	0.035
Winter	-0.041	-0.197	-0.202	-0.043	0.070	0.160
<b>RH</b>						
Spring	-0.371	-0.088	0.075	-0.245	-0.286	-0.270
Summer	-0.081	0.121	0.128	0.070	-0.302	-0.191
Fall	-0.383	0.009	0.093	-0.155	-0.320	-0.120
Winter	-0.218	-0.007	0.067	0.013	-0.179	-0.251
<b>TEMP</b>						
Spring	-0.168	-0.052	-0.241	-0.006	-0.071	0
Summer	0.065	-0.117	-0.053	0.111	0.227	0.083
Fall	-0.576	0.401	-0.489	-0.471	-0.334	0.294
Winter	-0.080	-0.134	-0.240	-0.094	0.041	0.431
<b>P</b>						
Spring	0.008	-0.025	0.017	-0.022	-0.174	-0.140
Summer	-0.210	-0.028	0	-0.125	-0.184	-0.256
Fall	0.175	0.116	0.050	-0.045	0.102	0.114
Winter	-0.178	-0.063	-0.036	-0.174	-0.142	-0.070

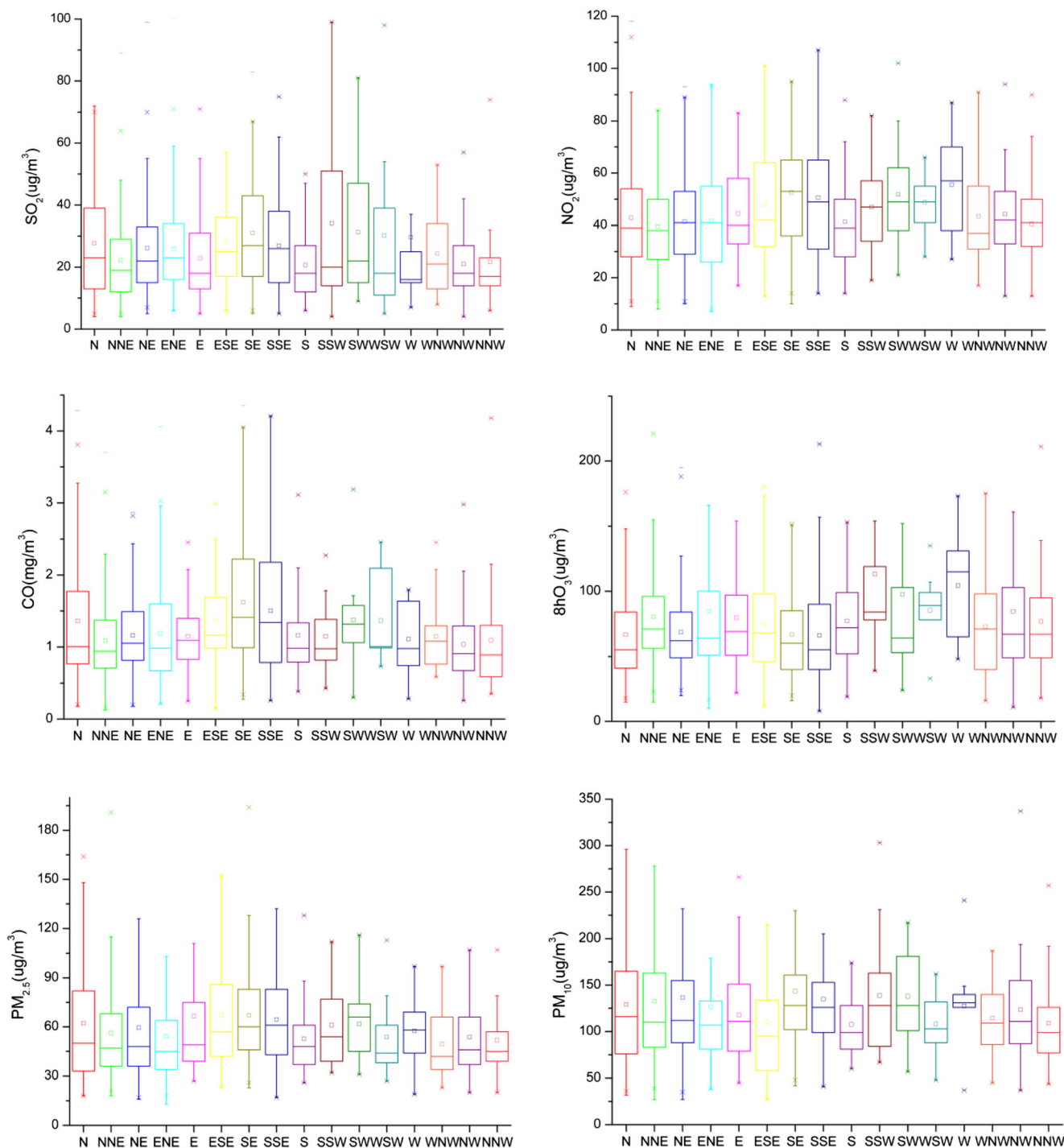


**Fig. 6** The concentrations of pollutants according to their respective wind directions

PM was the uppermost contaminant while in the East coastal regions,  $\text{O}_3$  was the uppermost contaminant.

Lanzhou had high PM year mean concentrations ( $113.5 \pm 21.3 \mu\text{g m}^{-3}$  for  $\text{PM}_{10}$  and  $48.8 \pm 12.3 \mu\text{g m}^{-3}$  for  $\text{PM}_{2.5}$ ), but was still in the state of moderate pollution. Only 6.2% cities exceeded the CAAQS Grade II standards for  $\text{SO}_2$  ( $60 \mu\text{g m}^{-3}$ ). Similar to  $\text{SO}_2$ , few cities are exceeding the CAAQS Grade II standards ( $4 \text{ mg m}^{-3}$  for CO), but

Lanzhou was in a relatively severe condition with CO pollution ranking in 16/113.  $\text{O}_3$  was in the state of moderate pollution compared with other regions. Lanzhou was  $46.9 \pm 8.2 \mu\text{g m}^{-3}$  year mean  $\text{NO}_2$  and in a severe pollution status (7/113).

From the comparisons with other Chinese cities,  $\text{NO}_2$  pollution was serious, followed by  $\text{PM}_{10}$  and CO, while  $\text{SO}_2$ ,  $\text{PM}_{2.5}$ , and  $\text{O}_3$  were relatively lighter in Lanzhou. The minor

pollution of SO<sub>2</sub> meant that mitigation measures to improve air quality in Lanzhou were implemented by local government, such as reducing industrial emissions. But the issue of NO<sub>2</sub> pollution suggested that more efforts should be taken to prioritize the resolution of traffic problem and improve diffusion conditions. PM<sub>10</sub> pollution was severe because Lanzhou was affected by surrounding Gobi Desert; thus, we need increase efforts to reduce the entrainment of dust.

### Relationship between air pollutants and meteorological parameters

The correlation coefficients (*R*) between six pollutants and four meteorological parameters during 2013–2016 were shown (Table 2). PM<sub>10</sub> has positive correlations with wind

**Table 3** Correlations of pollutants in Lanzhou based on daily data during 2013–2016

	PM <sub>10</sub>	SO <sub>2</sub>	CO	NO <sub>2</sub>	8-hO <sub>3</sub>
Yearly					
PM <sub>2.5</sub>	0.770	0.556	0.435	0.357	−0.148
PM <sub>10</sub>		0.321	0.188	0.241	0.006
SO <sub>2</sub>			0.598	0.427	−0.149
CO				0.697	−0.254
NO <sub>2</sub>					0.061
Spring					
PM <sub>2.5</sub>	0.906	0.348	−0.008	−0.030	−0.042
PM <sub>10</sub>		0.306	0.063	0.005	−0.008
SO <sub>2</sub>			0.444	0.441	−0.005
CO				0.674	−0.042
NO <sub>2</sub>					0.123
Summer					
PM <sub>2.5</sub>	0.746	0.477	0.348	0.273	−0.016
PM <sub>10</sub>		0.497	0.236	0.333	0.170
SO <sub>2</sub>			0.470	0.354	0.243
CO				0.554	0.200
NO <sub>2</sub>					0.421
Fall					
PM <sub>2.5</sub>	0.784	0.709	0.540	0.436	−0.206
PM <sub>10</sub>		0.500	0.350	0.356	−0.049
SO <sub>2</sub>			0.476	0.336	−0.291
CO				0.740	−0.133
NO <sub>2</sub>					0.185
Winter					
PM <sub>2.5</sub>	0.612	0.501	0.502	0.510	−0.016
PM <sub>10</sub>		0.243	0.310	0.438	0.063
SO <sub>2</sub>			0.402	0.353	0.108
CO				0.750	−0.178
NO <sub>2</sub>					0.011

speed (WS) in all seasons, which is due to flowing dust following the wind (Hu et al. 2008). However, the secondary pollutant O<sub>3</sub> has negative correlations with WS in the summer, but has positive correlations in other seasons. High WS removes fine particle leading to enhancement of the solar radiation, which increases O<sub>3</sub> formation (Atkinson 2000; Jacob and Winner 2009). Most pollutants have negative correlation with relative humidity (RH) in four seasons, except CO in the whole year and NO<sub>2</sub> and PM<sub>2.5</sub> in summer. Higher RH caused the formation of the more aerosol phase from semi-volatile compounds, which resulted in higher secondary pollutant concentrations and lower primary dominated pollutant concentrations (Jayamurugan et al. 2013). The correlations between pollutants and temperature were negative in all seasons except O<sub>3</sub> which is because temperatures play the important role in O<sub>3</sub> formation (Ran et al. 2009; Pusede et al. 2015). In conclusion, lower primary pollutants were associated with higher WS, but for O<sub>3</sub>, a secondary pollutant with special formation mechanism, lower concentrations were associated with depressed temperatures.

Figure 6 shows the concentrations of pollutants from their respective wind directions for better understanding of the influences of wind direction on the six pollutants. In Lanzhou, southeasterly wind led to the highest SO<sub>2</sub> concentrations, followed by northerly wind, while westerly wind resulted in the lowest SO<sub>2</sub> concentrations. Westerly wind was related to the highest NO<sub>2</sub> concentrations, followed by southeasterly wind. The highest CO concentrations were associated with southeasterly winds, but westerly wind led to the highest O<sub>3</sub> concentrations. Meanwhile, both the highest PM<sub>2.5</sub> and PM<sub>10</sub> concentrations were associated with westerly wind followed by southeasterly wind; northwesterly wind resulted in the lowest PM concentrations.

In general, the high concentrations of SO<sub>2</sub>, CO, PM<sub>2.5</sub>, and PM<sub>10</sub> were associated with easterly winds (east, southeast, and southwest winds), while O<sub>3</sub> had similar results with NO<sub>2</sub> and the maximum values were related to northerly and westerly winds. This is because north and westerly winds accompanied relatively a high intensity of cold air intrusion, resulting in good diffusion conditions (Ying et al. 2014; Zhang et al. 2012). However, the association between O<sub>3</sub> and NO<sub>2</sub> and westerly wind indicated the emissions from petrochemical and oil refinery industry in westerly Xigu District had contributions to air oxidation environment.

Air pollutants would be impacted by specific wind directions more than other wind directions for several reasons. On the one hand, the wind speed of a specific direction is smaller than those from other directions and it is beneficial to the enhancement of pollutants. On the other hand, in the upwind regions from specific directions, the pollutant emissions and precursors are larger than other areas, which lead to more pollutants transported.

**Table 4** Factor loadings from PCA in the four seasons

	Spring			Summer		Fall		Winter	
	1	2	3	1	2	1	2	1	2
SO <sub>2</sub>	0.404	<i>0.684</i>	0.016	<i>0.643</i>	0.417	<i>0.780</i>	−0.324	<i>0.653</i>	0.193
NO <sub>2</sub>	−0.077	<i>0.886</i>	0.170	0.259	<i>0.800</i>	<i>0.691</i>	<i>0.604</i>	<i>0.813</i>	−0.180
CO	−0.036	<i>0.882</i>	−0.194	0.373	<i>0.642</i>	<i>0.784</i>	0.270	<i>0.773</i>	−0.401
O <sub>3</sub>	−0.015	−0.004	<i>0.991</i>	−0.102	<i>0.781</i>	−0.191	<i>0.823</i>	0.053	<i>0.926</i>
PM <sub>2.5</sub>	<i>0.973</i>	0.016	−0.025	<i>0.924</i>	0.020	<i>0.899</i>	−0.183	<i>0.853</i>	0.036
PM <sub>10</sub>	<i>0.958</i>	0.051	0.000	<i>0.866</i>	0.129	<i>0.764</i>	−0.090	<i>0.693</i>	0.164
Variance (%)	37.934	29.882	17.469	47.205	20.892	52.143	21.027	47.924	18.419

The absolute values for factor loadings greater than 0.5 were italic

## Sources apportionment

### Relationship between air pollutants

The Pearson correlation coefficients ( $R$ ) were calculated between six air pollutants in different seasons during 2013–2016 (Table 3). Green represent positive correlation, while orange represent negative correlation, and the darker the color, the stronger the correlation. PM<sub>2.5</sub> was highly correlated ( $R > 0.500$ ) with PM<sub>10</sub> and SO<sub>2</sub>, suggesting that the common sources of species from burning of coal and biomass. CO was highly correlated with NO<sub>2</sub> and SO<sub>2</sub> (0.697 and 0.596, respectively), which probably meant that both fossil fuel and coal combustion could be related to the generation of CO. Meanwhile, the correlations between PM<sub>2.5</sub> and PM<sub>10</sub> in the spring ( $R = 0.906$ ) were stronger than those in the winter ( $R = 0.612$ ), and similar correlations between PM<sub>2.5</sub> and SO<sub>2</sub> were also observed. Correlation in the spring ( $R = 0.306$ ) is weaker than in the fall ( $R = 0.709$ ), which was due to the high sandstorms in the spring and the domestic heating in the fall. O<sub>3</sub> was weakly positively ( $0.000 < R < 0.299$ ) and weakly negatively ( $-0.300 < R < -0.001$ ) correlated with other pollutants. While O<sub>3</sub> became more positively correlated with other pollutants in the summer than in other seasons, especially with NO<sub>2</sub> ( $R = 0.421$ ). It is partially the result of the O<sub>3</sub> formation by photochemical reactions with increasing NO<sub>2</sub> level and favorable weather conditions. The correlations between PM correlations with CO and NO<sub>2</sub> gradually increased from the spring to the winter, which is likely due to the stronger formation of secondary PM in the winter (Berglen et al. 2004; Tie et al. 2006). It was meaningful that the correlation between PM<sub>2.5</sub> and CO was a little higher ( $R = 0.435$ ) than that between PM<sub>10</sub> and CO ( $R = 0.188$ ). Similar to PM and NO<sub>2</sub>, the correlation( $R$ ) between PM<sub>2.5</sub> and NO<sub>2</sub> is 0.357 while between PM<sub>10</sub> and NO<sub>2</sub> is 0.241. This implies that the gaseous pollutants emission process is accompanied by the emission of fine particles. In general, emissions

of SO<sub>2</sub>, NO<sub>2</sub>, and CO are often related to the emission of PM, and these gaseous pollutants are also accompanied by the generation of secondary aerosols, which are mainly fine particles. However, the correlation between O<sub>3</sub> and other pollutants is negative, and it is due to O<sub>3</sub> depletion during the oxidation process (Rypdal et al. 2009).

### Principal component analysis

Principal component analysis (PCA) is a widely used statistical technique, which can quantitatively identify several independent factors among the air pollutants. It can explain the data variance and apportion the sources by the eigenvector decomposition of a matrix of pair-wise correlations. In this study, PCA is used based on Kaiser's criterion, and orthogonal rotation (specifically VARIMAX rotation) is applied (Johnson and Wichern 1998) in Table 4.

In spring, three principal components (PC) accounted for 85.2% of the total variance. Thereinto, PC1 accounted for 37.9% of the total variance, with relatively high loading in PM<sub>2.5</sub> (0.973), PM<sub>10</sub> (0.958), and SO<sub>2</sub> (0.404), indicating its relation with stationary source emissions such as coal combustion, and high loading in PM<sub>2.5</sub> (0.973) and PM<sub>10</sub> (0.958), and moderate loading in SO<sub>2</sub> also shows the effects from the crustal and soil dust from sandstorm in spring. PC2 contained SO<sub>2</sub>, NO<sub>2</sub>, and CO with 29.9% of the total variance, which was associated with traffic emissions. PC3 was the ozone-specific component and accounted for 17.5% of the total variance. The ozone-specific component was highly associated with O<sub>3</sub> and NO<sub>2</sub> in summer and fall (both the principal component 2), indicating characteristic of reactivity in the NO<sub>x</sub>-O<sub>3</sub> system. In summer, two PC accounted for 68.1% of the total variance. PC1 had relatively highly positive contributions from PM<sub>2.5</sub> (0.924), PM<sub>10</sub> (0.866), and SO<sub>2</sub> (0.643), which could be explained by stationary source emissions from the activities in the industrial areas. PC2 was composed of NO<sub>2</sub>, CO, and O<sub>3</sub>, mainly from traffic emissions. In fall and winter,

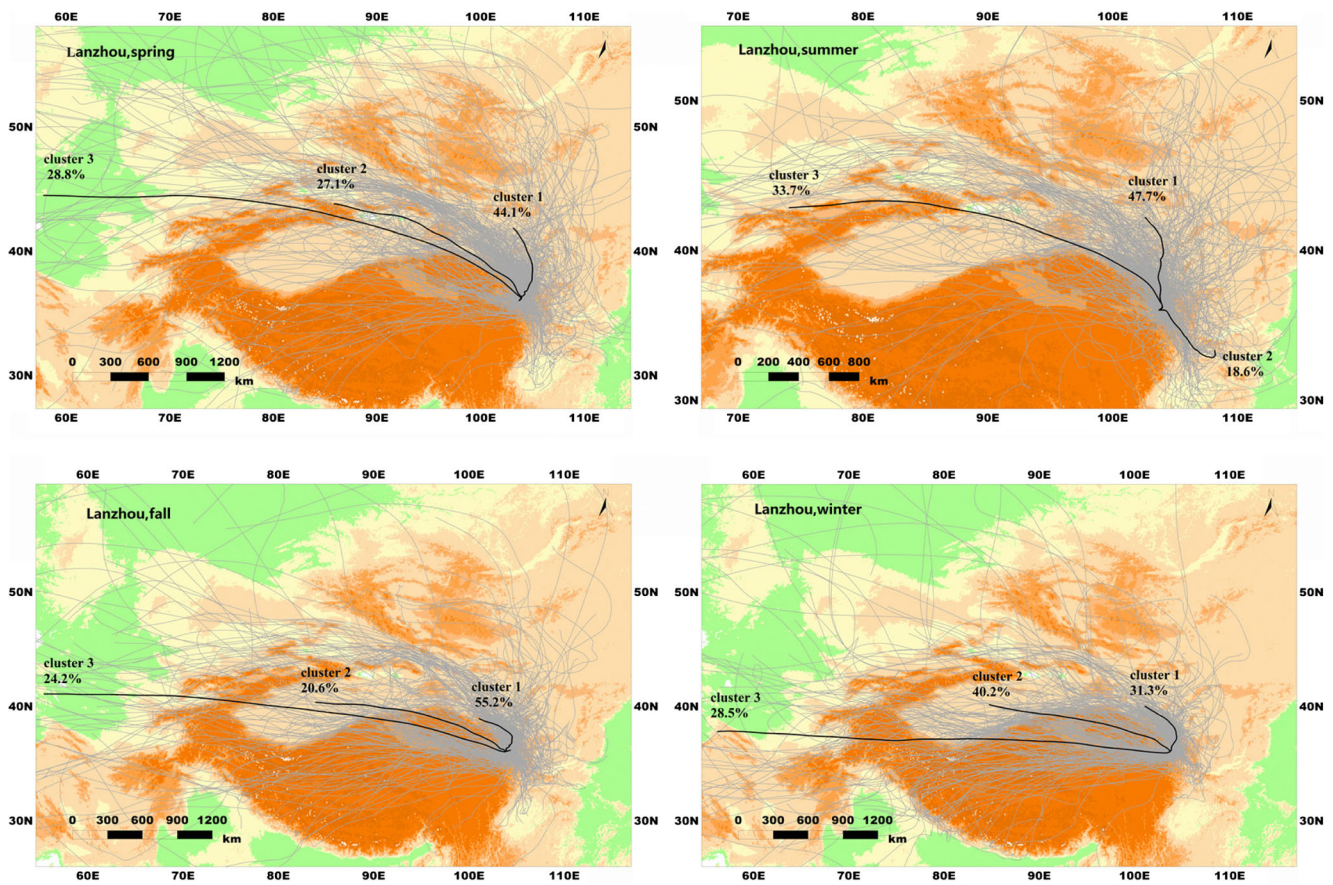


Fig. 7 Five-day back trajectory of air masses in Lanzhou during 2013–2016

two PC accounted for 73.2 and 66.3% of the total variance, respectively. PC1 accounted for 52.1 and 47.9% of the total variance, respectively, which could be explained by coal or fuel oil combustion emissions from heating due to the positive contribution from all the pollutants except O<sub>3</sub>. PC2 could be

relative to photochemical activity due to the positive combustion from O<sub>3</sub> and also NO<sub>2</sub> in fall which accounted for 21.0 and 18.4% of the total variance respectively in fall and winter. Heating activities had much more contributions than traffic emissions to air pollution in winter.

**Table 5** Statistics of average concentrations of gaseous pollutants for each type of air mass arriving in Lanzhou

Year	Air mass type	SO <sub>2</sub>	NO <sub>2</sub>	CO	O <sub>3</sub>	PM <sub>2.5</sub>	PM <sub>10</sub>
Spring	Cluster 1	20.7	43.8	950	107.4	57.0	142.3
	Cluster 2	23.7	44.7	1000	115.1	60.0	174.1
	Cluster 3	22.2	45.3	930	118.1	62.2	170.4
Summer	Cluster 1	14.2	42.4	970	116.7	42.5	94.7
	Cluster 2	15.3	33.0	910	97.6	46.7	104.4
	Cluster 3	16.8	42.0	960	133.3	43.5	107.5
Fall	Cluster 1	20.3	46.7	1220	83.0	55.0	124.1
	Cluster 2	24.5	45.8	1250	67.0	62.2	131.6
	Cluster 3	22.8	46.8	1390	86.1	59.6	127.4
Winter	Cluster 1	49.2	57.1	2070	78.1	84.1	140.7
	Cluster 2	34.3	55.2	1890	68.4	65.6	120.7
	Cluster 3	39.0	52.5	1890	68.5	74.1	148.0

**Table 6** Emission of waste gas and major pollutants in Lanzhou from 2012 to 2015( $10^4$  tons, except industrial waste gas 100 million  $m^3$ )

Year	Industrial waste gas	SO <sub>2</sub>			NO <sub>x</sub>			Soot		
		Total	Industrial	Living	Total	Industrial	Living	Total	Industrial	Living
2012	3954.42	8.04	6.87	1.17	10.70	8.38	2.32	3.60	3.36	0.24
2013	3954.00	7.96	7.22	0.74	8.57	8.38	0.19	4.31	4.20	0.11
2014	3168.04	7.40	6.76	0.64	6.88	6.60	0.28	6.98	6.42	0.56
2015	3576.57	6.97	6.12	0.85	5.42	5.14	0.28	5.08	4.52	0.56

### Back trajectory clustering analysis

The importance of long-range transport of air pollution has been gradually recognized in several decades (Meng et al. 2009). Based on the cluster analysis (Fig. 7), in all 4 years, air masses over the Lanzhou are from the Hexi Corridor and Inner Mongolia (cluster 1, 31.3–55.2%), the Taklimakan and Gobi Desert in Sinkiang (cluster 2, 20.6–40.2%, while in summer, 18.6% from the Southeast China with more moisture), and the Central Asia (cluster 3, 24.2–33.7%).

Air masses from different directions have different pollutant concentrations since the emission origins are unevenly distributed around the Lanzhou site. In order to characterize the pollutant levels from different air masses, daily mean concentrations of six pollutants for corresponding clusters of backward trajectories during 2013–2016 are summarized (Table 5). The SO<sub>2</sub>, CO, and PM<sub>2.5</sub> level consistent with cluster 1 was highest in winter than other seasons, together with the highest SO<sub>2</sub>, CO, and PM<sub>2.5</sub> level which occurred in wintertime (see section “Temporal variation of air pollutants”), which suggested that pollutants from the Hexi Corridor and Inner Mongolia contributed most significantly to the higher SO<sub>2</sub>, CO, and PM<sub>2.5</sub> level. The NO<sub>2</sub> level corresponding to cluster 1 in summer and winter would be a little higher than other seasons due to Hexi Corridor and Inner Mongolia which probably contributed to the higher NO<sub>2</sub>. The O<sub>3</sub> level corresponding to cluster 3 was highest in summer, which pointed that the Central Asia effected the O<sub>3</sub> level. The PM<sub>10</sub> level corresponding to cluster 2 and cluster 3 was highest in spring and winter, respectively, suggesting that the higher PM<sub>10</sub> level in Lanzhou was influenced by the air masses from the desert areas of the Sinkiang and the Central Asia.

### Cause analysis

The temporal distribution of pollutants is affected mainly by meteorological conditions and anthropogenic sources (e.g., population and traffic density). These two major factors were analyzed in this study.

### Local emissions

Emission of waste gas and major pollutants in Lanzhou from 2012 to 2015 was in Table 6. The industrial waste gas emission was  $3.96 \times 10^{11} m^3$  in 2012 and  $3.58 \times 10^{11} m^3$  in 2015. From 2012 to 2015, it decreases to  $3.78 \times 10^{10} m^3$ . SO<sub>2</sub> emissions decreased from  $8.04 \times 10^4$  tons to  $6.97 \times 10^4$  tons, and NO<sub>x</sub> emissions decreased from  $10.70 \times 10^4$  tons to  $5.42 \times 10^4$  tons during 2012–2015. The possibility is that increasingly stringent air quality management strategies and emission control standards from government have resulted in decrease of localized emissions, including reducing stationary emissions (renovating pollution industries, central heating), “odd-even” traffic restriction, watering on the streets, further promoting green travel, replacing coal with natural gas, and increasing vegetative cover to reduce secondary dust (Zhao et al. 2013). On the other hand, soot emissions increased from  $3.60 \times 10^4$  tons in 2012 to  $5.08 \times 10^4$  tons in 2015, and it is likely that the pollution emission sources have become more dispersed.

### Meteorological condition

As we know, enhanced concentrations of atmospheric aerosol and some gaseous pollutants usually occur in urban areas during specific meteorological conditions (i.e., temperature inversion, pressure system, and low wind effect) (Zhang et al. 2015; He et al. 2017). In addition, pollution in the boundary layer of urban areas can also be influenced by local, regional sources, or their combined effects (Choi et al. 2008). Using the generalized linear regression model (GLM), Liang et al. (2017) found that the meteorological conditions and pollution control strategies contributed 30 and 28% to the reduction of the PM<sub>2.5</sub> concentration during APEC and 38 and 25% during the Victory Parade, respectively.

Our study demonstrates that during the period of 2013 to 2015, both wind speed and temperature in Lanzhou showed an overall decrease with a rate of  $6.7 \times 10^{-5} m s^{-1} year^{-1}$  and  $0.0002 \text{ } ^\circ C year^{-1}$ , respectively, while RH increased with a rate of  $0.0015\% year^{-1}$ .

These slight variations obviously should have little effects on pollutant concentrations in general. The annual happen time of the north dust weather in the spring presents slowly descend tendency (Chu et al. 2008c; Fig. S2 in the supplement), which might lead to the decreased PM. As a matter of fact, the effect and interaction mechanism between meteorological factors and pollutant concentrations in Lanzhou remain largely unknown; thus, a further study including multi-scale circulation investigation and model simulation should be employed.

## Conclusion

The air quality is improving in Lanzhou valley, a petrochemical industrialized city located in the Loess Plateau, and even “Lanzhou Blue” has appeared. Airborne pollutant characteristics, potential sources, and causes are studied from January 2013 to December 2016. Major conclusions are as follows:

SO<sub>2</sub>, PM<sub>10</sub>, and PM<sub>2.5</sub> present decreasing trends while NO<sub>2</sub>, CO, and O<sub>3</sub> present increasing trends. The concentrations of pollutants were signally higher in the winter (~12:00) than those in other seasons, but high O<sub>3</sub> level appeared in summer (~16:00). PM<sub>10</sub> has a high concentration in spring due to the sandstorms. Compared with air pollutant concentrations in other Chinese cities, NO<sub>2</sub> and PM<sub>10</sub> were relatively severe in Lanzhou. Relationship between air pollutants and meteorological parameters suggested that higher wind speed from north and west was related to lower primary pollutants, but elevated temperature was related to the higher secondary pollutant O<sub>3</sub> concentrations.

Source apportionment suggested that Lanzhou was influenced by coal and biomass combustion mainly in the winter, long-distance transport of sand-dust from the Central Asia mainly in the spring, and the secondary aerosol formation in all the seasons. In addition to geographical locations, the improvement of air quality in Lanzhou valley was probably related to the variations of local emissions and meteorological condition. Emissions had a decreasing trend in recent years, which is achieved by the increasingly stringent air quality management strategies and emission control standards from the government. The temporal distribution of pollutants that affected meteorological conditions in Lanzhou remains largely unknown; thus, a further study should be employed.

**Acknowledgements** The authors wish to thank Prof. Li for the invaluable comments and Qingyue Open Environmental Data Center for the support on environmental data processing.

**Funding** The work was supported by the SKLCS FUNDING (grant number SKLCS-ZZ-2017), National Natural Science Foundation of China (grant number 41471058), and the NSFC project (grant number 91425303).

## References

- Atkinson R (2000) Atmospheric chemistry of VOCs and NO<sub>x</sub>. *Atmos Environ* 34:2063–2101
- Atkinson R, Arey J (2003) Atmospheric degradation of volatile organic compounds. *Chem Rev* 103:4605–4638
- Berglen TF, Berntsen TK, Isaksen ISA et al (2004) A global model of the coupled sulfur/oxidant chemistry in the troposphere: the sulfur cycle. *J Geo-Phys Res-Atmos* 109(19):2083–2089. <https://doi.org/10.1029/2003JD003948>
- Chan C, Yao X (2008) Air pollution in mega cities in China. *Atmos Environment* 42(24):1–42
- Choi H, Zhang Y, Kim K (2008) Sudden high concentration of TSP affected by atmospheric boundary layer in Seoul metropolitan area during dust storm period. *Environ Int* 34:635–647
- Chu PC, Chen Y, Lu S (2008a) Afforestation for reduction of NO<sub>x</sub> concentration in Lanzhou China. *Environ Int* 34(5):688–697
- Chu PC, Chen Y, Lu S (2008b) Atmospheric effects on winter SO<sub>2</sub> pollution in Lanzhou, China. *Atmos Res* 89(4):365–373
- Chu PC, Chen Y, Lu S (2008c) Particulate air pollution in Lanzhou China. *Environ Int* 34(5):698–731
- Draxler RR, Rolph GD 2013 HYSPLIT (Hybrid Single-Particle Lagrangian Integrated Trajectory) model access via NOAA ARL READY. NOAA Air Resources Laboratory, Silver Spring, MD. Available at: <http://www.arl.noaa.gov/HYSPLIT.php>
- Gansu Yearbook 2016 China Statistic Press, Beijing. <http://www.gstj.gov.cn/w/Default.htm>
- Guan QY, Cai A, Wang FF, Yang LQ, Xu CQ, Liu ZY (2017) Spatio-temporal variability of particulate matter in the key part of Gansu Province, western China. *Environ Pollut* 230:189–198
- He KB, Yang FM, Ma YL et al (2001) The characteristics of PM<sub>2.5</sub> in Beijing, China. *Atmos Environ* 35:4959–4970
- He JJ, Gong SL, Yu Y et al (2017) Air pollution characteristics and their relation to meteorological conditions during 2014–2015 in major Chinese cities. *Environ Pollut* 223:484–496
- Hu XM, Zhang Y, Jacobson MZ, Chan CK (2008) Coupling and evaluating gas/particle mass transfer treatments for aerosol simulation and forecast. *J Geophys Res* 113(D11):3078–3078. <https://doi.org/10.1029/2007JD009588>
- Hu J, Wang Y, Ying Q, Zhang H (2014) Spatial and temporal variability of PM<sub>2.5</sub> and PM<sub>10</sub> over the North China Plain and the Yangtze River Delta, China. *Atmos Environ* 95:598–609
- IPCC: Climate change (2007) The physical science basis, Contribution of Working Group I to the Fourth Assessment Report of the IPCC 978 0521 88009-1; 2007 [Hardback; 978 0521 70596-7 paperback]
- Jacob DJ, Winner DA (2009) Effect of climate change on air quality. *Atmos Environ* 43:51–63. <https://doi.org/10.1016/j.atmosenv.2008.09.051>
- Jayamurugan R, Kumaravel B, Palanivelraja S, Chockalingam MP (2013) Influence of temperature, relative humidity and seasonal variability on ambient air quality in a coastal urban area. *Int J Atmos Sci* 2013(9):1–7. <https://doi.org/10.1155/2013/264046>
- Johnson RA, Wichern D (1998) Applied multivariate statistical analysis. Prentice Hall, Englewood Cliffs
- Kan H, London S, Chen G (2007) Differentiating the effects of fine and coarse particles on daily mortality in Shanghai, China. *Environ Int* 33(3):376–384
- Liang PF, Zhu T, Fang YH et al (2017) The role of meteorological conditions and pollution control strategies in reducing air pollution in Beijing during APEC 2014 and Victory Parade 2015. *Atmos Chem Phys* 17:13921–13940
- Lim SS, Vos T, Flaxman AD et al (2013) A comparative risk assessment of burden of disease and injury attributable to 67 risk factors and risk factor clusters in 21 regions, 1990–2010: a systematic analysis for

- the Global Burden of Disease Study 2010. *Lancet* 380(9859):2224–2260
- Liu Z, Hu B, Wang L (2015) Seasonal and diurnal variation in particulate matter (PM<sub>10</sub> and PM<sub>2.5</sub>) at an urban site of Beijing: analyses from a 9-year study. *Environ Sci Pollut Res* 22:627–642. <https://doi.org/10.1007/s11356-014-3347-0>
- Meng ZY, Xu XB, Yan P et al (2009) Characteristics of trace gaseous pollutants at a regional background station in Northern China. *Atmos Chem Phys* 9(3):927–936
- Ostro B (2004) Outdoor air pollution: assessing the environmental burden of disease at national and local levels. World Health Organization, WHO Environmental Burden of Disease, Geneva Series, No. 5
- Pusede SE, Steiner AL, Cohen RC (2015) Temperature and recent trends in the chemistry of continental surface ozone. *Chem Rev* 115(10):650–659. <https://doi.org/10.1021/cr5006815>
- Ran L, Zhao C, Geng F, Tie X, Tang X, Peng L, Zhou G, Yu Q, Xu J, Guenther A (2009) Ozone photochemical production in urban Shanghai, China: analysis based on ground level observations. *J Geophys Res* 114(D15):4228–4240. <https://doi.org/10.1029/2008JD010752>
- Rypdal K, Rive N, Berntsen T, Fagerli H, Klimont Z, Mideksa TK, Fuglestad JS (2009) Climate and air quality-driven scenarios of ozone and aerosol precursor abatement. *Environ Sci Pol* 12:855–869
- Ta W, Wang T, Xiao H (2004) Gaseous and particulate air pollution in the Lanzhou Valley, China. *Sci Total Environ* 320:163–176
- Tang XY, Li JL, Dong ZX (1989) Photochemical pollution in Lanzhou, China—a case study. *J Environ Sci* 58(1):384–395
- Tie X, Brasseur GP, Zhao C, Granier C, Massie S, Qin Y, Wang PC, Wang G, Yang PC, Richter A (2006) Chemical characterization of air pollution in Eastern China and the Eastern United States. *Atmos Environ* 40:2607–2625
- Timonen H, Wigder N, Jaffé D (2013) Influence of background particulate matter (PM) on urban air quality in the Pacific Northwest. *J Environ Manag* 129:333–340
- Titos G, Lyamani H, Pandolfi M, Alastuey A, Alados-Arboledas L (2014) Identification of fine (PM<sub>1</sub>) and coarse (PM<sub>10-1</sub>) sources of particulate matter in an urban environment. *Atmos Environ* 89:593–602
- Wang F 2011 Pollution characteristics and formation causes of atmospheric particles and its chemical components in Lanzhou City (PhD thesis in Chinese) Lanzhou University, Lanzhou
- Wang YQ, Zhang XY, Arimoto R et al (2004) The transport pathways and sources of PM<sub>10</sub> pollution in Beijing during spring 2001, 2002 and 2003. *Geophys Res Lett* 31(14):L14110. <https://doi.org/10.1029/2004GL019732>
- Wang S, Feng X, Zeng X, Ma Y, Shang K (2009) A study on variations of concentrations of particulate matter with different sizes in Lanzhou, China. *Atmos Environ* 43:2823–2828
- Wang YG, Ying Q, Hu J, Zhang H (2014) Spatial and temporal variations of six criteria air pollutants in 31 provincial capital cities in China during 2013–2014. *Environ Int* 73:413–422
- Wang YN, Jia C, Tao J (2016) Chemical characterization and source apportionment of PM<sub>2.5</sub> in a semi-arid and petrochemical-industrialized city, Northwest China. *Sci Total Environ* 573:1031–1040
- WHO 2016 URL [http://www.who.int/phe/health\\_topics/outdoorair/databases/en/](http://www.who.int/phe/health_topics/outdoorair/databases/en/)
- Xia XA, Chen HB, Wang PC, Zhang WX, Goloub P, Chatenet B, Eck TF, Holben BN (2006) Variation of column-integrated aerosol properties in a Chinese urban region. *J Geophys Res* 111:D05204. <https://doi.org/10.1029/2005JD006203>
- Ying Q, Wu L, Zhang H (2014) Local and inter-regional contributions to PM<sub>2.5</sub> nitrate and sulfate in China. *Atmos Environ* 94:582–592
- Zhang QF, Crooks R (2012) Toward an environmentally sustainable future: country environmental analysis of the People's Republic of China. The Asian Development Bank, Mandaluyong City
- Zhang H, Li J, Ying Q, Yu JZ, Wu D, Cheng Y, He K, Jiang J (2012) Source apportionment of PM<sub>2.5</sub> nitrate and sulfate in China using a source-oriented chemical transport model. *Atmos Environ* 62:228–242
- Zhang HL, Wang YG, Hu JL et al (2015) Relationships between meteorological parameters and criteria air pollutants in three megacities in China. *Environ Res* 140:242–254
- Zhao PS, Dong F, He D et al (2013) Characteristics of concentrations and chemical compositions for PM<sub>2.5</sub> in the region of Beijing, Tianjin, and Hebei, China. *Atmos Chem Phys* 13(9):4631–4644. <https://doi.org/10.5194/acpd-13-863-2013>
- Zhao SP, Yu Y, Yin DY, He JJ, Liu N, Qu JJ, Xiao JH (2016) Annual and diurnal variations of gaseous and particulate pollutants in 31 provincial capital cities based on in situ air quality monitoring data from China National Environmental Monitoring Center. *Environ Int* 86:92–106